



Nighttime medium-scale traveling ionospheric disturbances detected by network GPS receivers in Taiwan

C. C. Lee,¹ Y. A. Liou,² Y. Otsuka,³ F. D. Chu,⁴ T. K. Yeh,⁵
K. Hoshinoo,⁶ and K. Matunaga⁶

Received 3 April 2008; revised 28 September 2008; accepted 6 November 2008; published 31 December 2008.

[1] The nighttime medium-scale traveling ionospheric disturbances (MSTIDs) are detected by the network GPS receivers in Taiwan for the first time. The two-dimensional mapping technique (a spatial resolution of $0.05^\circ \times 0.05^\circ$ in latitude and longitude with 5×5 pixels smoothing) is applied on the data of TEC perturbations (TECp) and GPS phase fluctuations ($\Delta\text{TEC}/\text{min}$). The results show that the MSTIDs move southwestward to latitude of 20.5°N with a horizontal velocity between 100 and 160 m/s and a wavelength of about 500 km. The wavefronts of the MSTIDs are aligned along the northwest-southeast direction. Furthermore, the greater $|\Delta\text{TEC}/\text{min}|$ values are corresponding to the wave peak and trough of TECp. This coincidence indicates that the MSTIDs play an important role for the generation of *F* region irregularities in the low-latitude ionosphere.

Citation: Lee, C. C., Y. A. Liou, Y. Otsuka, F. D. Chu, T. K. Yeh, K. Hoshinoo, and K. Matunaga (2008), Nighttime medium-scale traveling ionospheric disturbances detected by network GPS receivers in Taiwan, *J. Geophys. Res.*, *113*, A12316, doi:10.1029/2008JA013250.

1. Introduction

[2] Medium-scale traveling ionospheric disturbances (MSTIDs), the mesoscale wave-like perturbation of the ionospheric plasma, are often observed in the ionospheric *F* region at midlatitudes. They have horizontal wavelength of several hundred kilometers, period of 15–60 min, and horizontal velocity of 100–250 m/s (see *Hunsucker* [1982] for a review). According to the previous studies [*Shiokawa et al.*, 2003a; *Hernández-Pajares et al.*, 2006; *Kotake et al.*, 2006, 2007], the daytime MSTIDs occur frequently in winter; while the nighttime MSTID most active near June solstice at the Japanese and Australian longitudinal sector and near December solstice in the European longitudinal sector.

[3] Since mid-1990s, the two-dimensional mapping technique using network GPS receivers has been used to reveal the characteristics of MSTIDs. First, *Saito et al.* [1998] used the high-resolution mapping of total electron content perturbations (TECp) observed by the GEONET (GPS Earth Observation Network) in Japan to show a spatial structure of the nighttime MSTIDs. Then, the two-dimensional TECp maps of the nighttime MSTIDs in Japan are compared with

the two-dimensional 630-nm airglow maps by *Saito et al.* [2001] and *Ogawa et al.* [2002], in which they found that these two maps are coincident with each other. In addition to the results in Japan, this mapping technique is recently applied on the features of the daytime and nighttime MSTIDs in North America [*Kotake et al.*, 2007; *Tsugawa et al.*, 2007]. Moreover, *Saito et al.* [2001] reported that the coherent echoes from the 3-m scale *F* region field-aligned irregularities (FAIs) were observed by the MU radar in the nights when the MSTIDs activity was high. Further, the horizontal distribution of the 3-m scale *F* region FAIs and TECp were examined by *Saito et al.* [2002], in which they found that both the TECp (MSTIDs) and *F* region FAIs propagated southwestward in the same velocity, and the regions where the echoes from the *F* region FAIs were detected correspond to the peak and the northeastern slope of TECp.

[4] Although the MSTIDs characteristics in the midlatitude ionosphere have been studied by many works, the low-latitude MSTIDs using the two-dimensional TECp mapping technique is not done yet. This study produces the two-dimensional TECp maps to investigate the nighttime MSTIDs in the low-latitude ionosphere for the first time. It is also the first attempt to apply the two-dimensional map technique on the data of GPS phase fluctuations [*Aarons et al.*, 1997; *Mendillo et al.*, 2000] to examine the horizontal distribution of *F* region irregularities. The TEC data are obtained from the network GPS receivers of National Land Surveying and Mapping Center (NSLC), the Ministry of the Interior, Taiwan.

2. Data Analysis

[5] In this study, the nighttime MSTIDs on 26 May 2006 are analyzed. For this day, the TEC data of 51 NSLC GPS

¹General Education Center, Ching Yun University, Jongli, Taiwan.

²Center for Space and Remote Sensing Research, National Central University, Chung-Li, Taiwan.

³Solar-Terrestrial Environment Laboratory, Nagoya University, Toyokawa, Japan.

⁴National Standard Time and Frequency Laboratory, Telecommunication Laboratories, Chunghwa Telecom Co., Ltd., Chung-Li, Taiwan.

⁵Institute of Geoinformatics and Disaster Reduction Technology, Ching Yun University, Jongli, Taiwan.

⁶Electronic Navigation Research Institute, Tokyo, Japan.

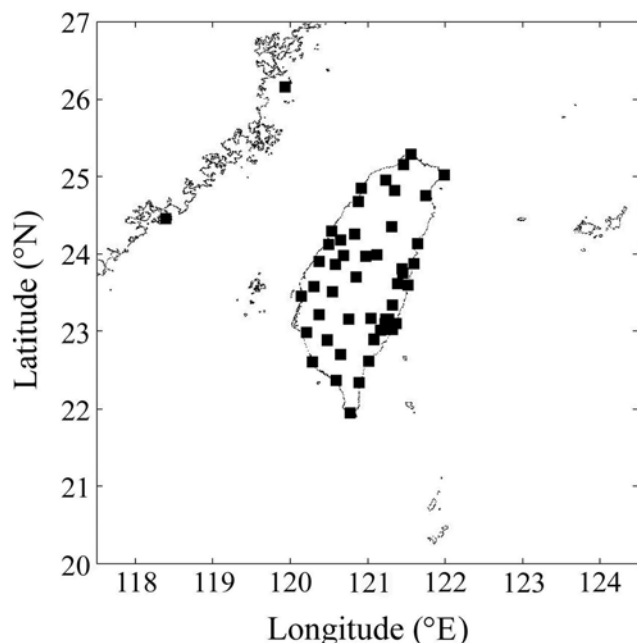


Figure 1. Distribution of GPS receivers operated by NSLC on 26 May 2006. Filled squares represent the locations of the GPS receivers.

receivers with a 30-s time resolution are used to produce the two-dimensional TECp map. The locations of the 51 GPS receivers are displayed in Figure 1. It is noted that the total number of NSLC GPS receivers is more than 85 in December 2007. All NSLC stations are equipped with dual-frequency GPS receivers, which provide the data of carrier phase and pseudo-range measurements at two frequencies ($f_1 = 1575.42$ MHz, $f_2 = 1227.60$ MHz).

[6] The slant TEC, I_s , which is the total number of electrons along the entire line-of-sight (LOS) between receiver and satellite, can be estimated using the following equation [Mannucci *et al.*, 1999]:

$$I_s = \frac{1}{40.3} \frac{f_1^2 f_2^2}{f_1^2 - f_2^2} [(L_1 - L_2) - (\lambda_1 n_1 - \lambda_2 n_2) + b_r + b_s],$$

where L_1 and L_2 are the carrier phases of the signal (converted to distance units), $\lambda_1 n_1$ and $\lambda_2 n_2$ are the integer cycle ambiguities, and b_r and b_s are the instrumental biases of receiver and satellite. The TECp, formed by MSTIDs, are obtained by subtracting one-hour running average of I_s from I_s for each LOS (see Saito *et al.* [1998, 2001] for details). The GPS phase fluctuations ($\Delta\text{TEC}/\text{min}$), caused by the F region irregularities of about 6 or longer kilometers scale size, are derived from the rate of change of TEC per minute (see Aarons *et al.* [1997] and Mendillo *et al.* [2000] for details). To eliminate changes in TEC which occur on timescale longer than 25 min, the 51-point high-pass filter is employed in the $\Delta\text{TEC}/\text{min}$ analysis. It is noted that the $|\Delta\text{TEC}/\text{min}|$ is used to calculate two indices of GPS phase fluctuations (see Mendillo *et al.* [2000] for details). Then, the TECp data are averaged with its nearly 24 grids (5×5 pixels smoothing) to make a two-dimensional TECp map. The size of each pixel is $0.05^\circ \times 0.05^\circ$ in latitude and longitude. The value for each pixel is an average of TECp

for all LOS which cross the pixel at 350 km altitude in 5 min. The 350 km altitude is the approximate F-peak height at 1400 UT on 26 May 2006, predicted by the IRI-2001 model [Bilitza, 2001]. The two-dimensional $|\Delta\text{TEC}/\text{min}|$ map is also produced in a spatial resolution of $0.05^\circ \times 0.05^\circ$ in latitude and longitude with 5×5 pixels smoothing. Because this study focuses on the TECp and $|\Delta\text{TEC}/\text{min}|$, the integer cycle ambiguities and instrumental biases would not affect the results of two-dimensional maps of TECp and $|\Delta\text{TEC}/\text{min}|$. Moreover, in order to prevent the uncertainties and cycle slips, the data from elevation angles lower than 60° are not included in this study.

3. Results and Discussion

[7] Figure 2 shows the time sequence of two-dimensional TECp maps during 1440–1530 UT (2240–2330 LT) on 26 May 2006, with a 10-min interval. The K_p index during this day ranges between 0+ and 1+, indicating that the geomagnetic activity is quiet. The plots are made using TEC data from two GPS satellites: PRN03 and PRN19. In Figure 2, it is found that the TECp structures derived with different satellites and elevation angles are consistent with each other. This demonstrates the altitude of 350 km used in data analysis is reasonable. At 1440 UT (Figure 2a), the wave-like structures appear in $119\text{--}122^\circ\text{E}$ and $21\text{--}26^\circ\text{N}$. Then, this wave-like structures move southwestward over Taiwan with a horizontal velocity of 100–160 m/s and a wavelength of about 500 km. The wavefronts of these structures are aligned along the northwest–southeast direction. Based on the horizontal velocity and wavelength, these wave-like structures are categorized as MSTIDs [Hunsucker, 1982]. Further, these characteristics are similar to the results previously observed in Japan [Saito *et al.*, 1998, 2001] and America [Kotake *et al.*, 2007; Tsugawa *et al.*, 2007]. Although at low latitudes, Ding *et al.* [2007] have observed the TIDs during a storm using GPS data, the TIDs that they found is the large-scale TIDs, which have a horizontal wavelength of more than 1000 km and periods of 30–180 min [Hunsucker, 1982]. Therefore, this MSTIDs event in the low-latitude ionosphere is detected by the GPS network for the first time.

[8] The nighttime MSTIDs are also recorded by the all-sky airglows imager in Yonaguni Island, Japan (24.5°N , 123°E) [Ogawa *et al.*, 2008]. Figure 3 displays the two-dimensional map of 630-nm airglow intensity perturbation observed by the Yonaguni imager at 1457 UT on 26 May 2006. The airglow structures show a significant coincidence with those of TECp at 1500 UT (Figure 2c). This coincidence reveals that the data processes (a spatial resolution of $0.05^\circ \times 0.05^\circ$ in latitude and longitude with 5×5 pixels smoothing) in this study are suitable for detecting the MSTIDs features. According to Kubota *et al.* [2000] and Ogawa *et al.* [2002], the emission rate of 630-nm airglow reaches a maximum value at 250–260 km, where is below the F-peak height. Therefore, this coincidence demonstrates that these nighttime MSTIDs occur mainly in the bottomside of the F region. In Figure 2c, the peak-to-peak amplitude of the TECp variations is about 3 TECU (1 TECU = 10^{16} ele/m²). At 1400 UT and 1600 UT on 26 May 2006, the background values of TEC at 120°E and 25°N are, respectively, 15 and 13 TECU, obtained from Global Ionosphere Maps (GIM) of

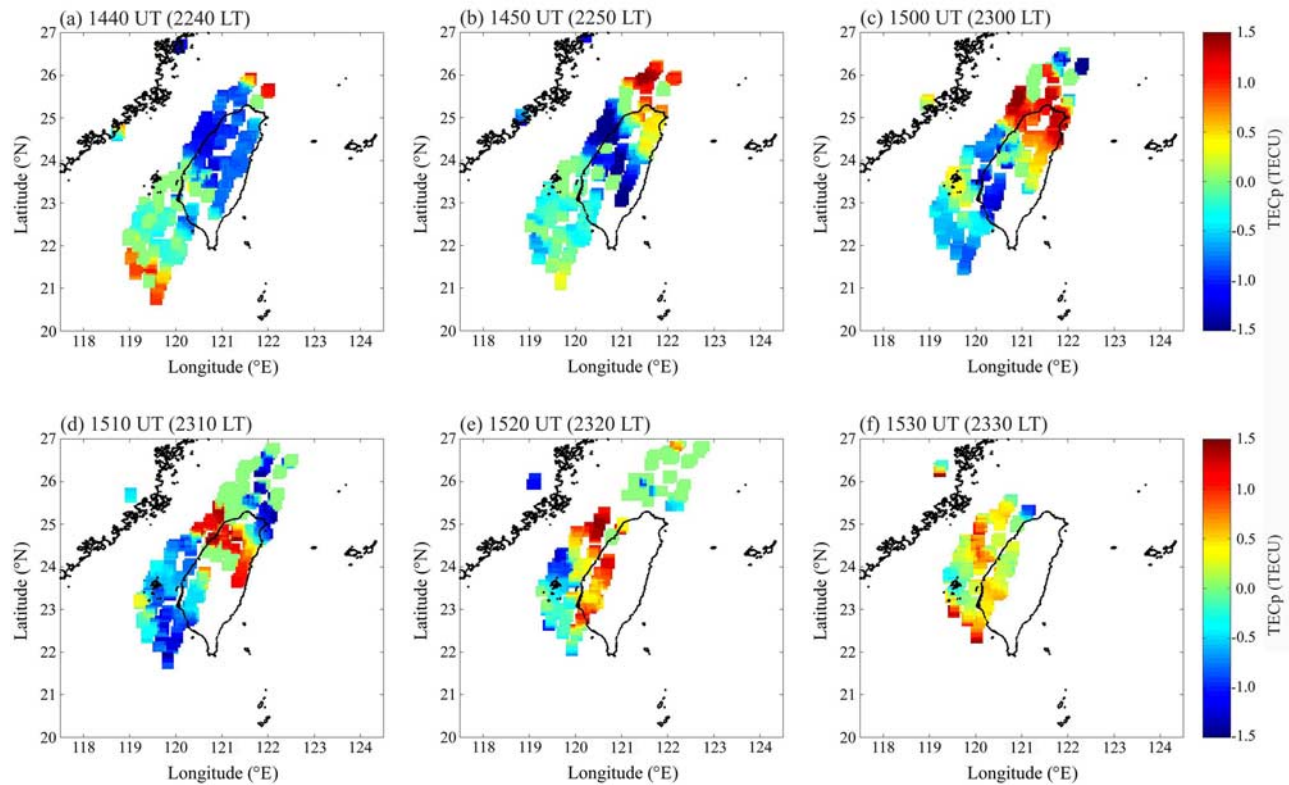


Figure 2. Time sequence of two-dimensional TECp maps during 1440–1530 UT (2240–2330 LT) on 26 May 2006, with a 10-min interval. The TEC data are obtained from two GPS satellites: PRN03 and PRN19.

CODE (Center for Orbit Determination in Europe). The ratio of TECp to the background TEC is about 10%, which is smaller than the amplitudes of airglow variations of about 20% (as shown in Figure 3). This result again indicates that the perturbations of ionospheric electron density take place mainly in the bottomside of *F* region [e.g., Saito *et al.*, 2001].

[9] In the previous studies, the polarization electric fields have been found inside the structure of nighttime MSTIDs [Saito *et al.*, 2002; Shiokawa *et al.*, 2003b]. Those results indicate that the Perkins instability could be the major mechanism in the generation of nighttime MSTIDs [Perkins, 1973; Garcia *et al.*, 2000]. Recently, Yokoyama *et al.* [2008] used a three-dimensional model of Perkins instability to simulate the northwest–southeast alignment of density perturbation. Nevertheless, the Perkins instability cannot explain the generation of nighttime MSTIDs well [e.g., Shiokawa *et al.*, 2003b]. According to the earlier studies, the atmospheric gravity wave [e.g., Hunsucker, 1982], as well as electrodynamic coupling between *F*- and *E* regions [e.g., Otsuka *et al.*, 2007] and between two hemispheres [e.g., Otsuka *et al.*, 2004; Shiokawa *et al.*, 2005] could be the seeds of the instability, too.

[10] Based on Ogawa *et al.* [2008], it is known that the nighttime MSTIDs in this study propagated southwestward from somewhere at latitudes higher than 46°N (the northernmost latitude of Japan) to 20.5°N. This result differs from the observed results on 4 and 6 August 1999 of Shiokawa *et al.* [2002]. Shiokawa *et al.* [2002] analyzed the 630 nm airglows of Okinawa (26.9°N, 128.3°E) CCD imager during 4–15 August 1999, and suggested that the southern limit of the southwestward propagation of MSTID

from the mainland Japan was possible around latitude of 28°N. The southern limit could be caused by the higher electron density that might prevent the atmospheric gravity wave, a seed of the wave-like structure of MSTIDs, propagation through the ion-drag effect [Shiokawa *et al.*, 2002, 2005]. Here, we examine the time constant (τ) for ion-drag given by $\tau = n/(N\nu_{in})$, where n , N , and ν_{in} are the neutral and ion densities, and the ion-neutral collision frequency. Based on

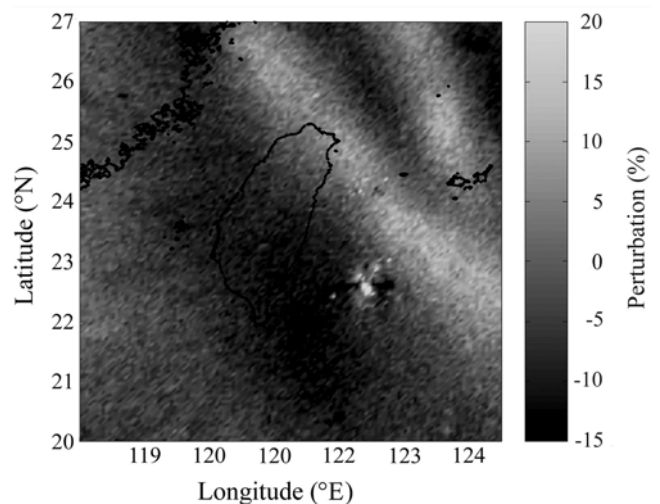


Figure 3. Two-dimensional maps of 630-nm airglow intensity perturbation at 1457 UT on 26 May 2006, observed by the Yonaguni CCD imager.

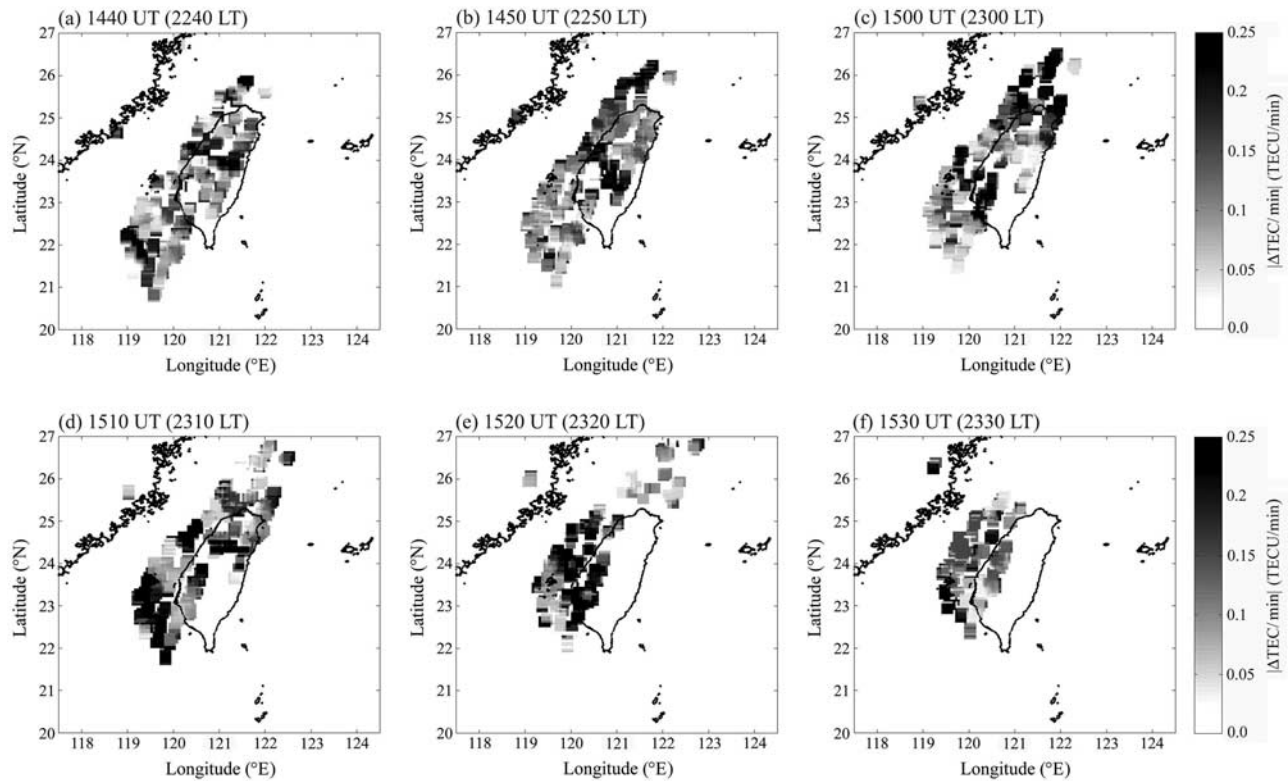


Figure 4. Time sequence of two-dimensional $|\Delta\text{TEC}/\text{min}|$ maps during 1440–1530 UT (2240–2330 LT) on 26 May 2006, with a 10-min interval. The TEC data are obtained from two GPS satellites: PRN03 and PRN19.

Liu and Yeh [1969] and Hines [1972], the atmospheric gravity wave would be damped by the ion-drag effect, when the value of $2\pi\tau$ is comparable to the period of gravity wave. Further, we calculate the value of τ at 1300 UT on 6 August 1999 and 26 May 2006. At 1300 UT on 6 August 1999, the value of N is $1.19 \times 10^{12} \text{ m}^{-3}$ at 350 km at 121°E and 25°N modeled by IRI-2001. The corresponding n value obtained from MSISE-90 model [Hedin, 1991] is $3.31 \times 10^{14} \text{ m}^{-3}$. The ν_{in} is $2.62 \times 10^{-1} \text{ sec}^{-1}$ estimated by the equation of $\nu_{\text{in}} = 2.4 \times 10^{-11} T^{0.5} n$ [Strobel and McElroy, 1970], where T , obtained from MSISE-90 model, is the atmospheric temperature in Kelvin. Then, the τ value at 1300 UT on 6 August 1999 is 1062 s (about 18 min). At 1300 UT on 26 May 2006, the τ value is 3973 s (about 66 min) calculated from n of $9.01 \times 10^{13} \text{ m}^{-3}$, N of $3.76 \times 10^{11} \text{ m}^{-3}$, and ν_{in} of $6.03 \times 10^{-2} \text{ sec}^{-1}$. The value of τ at 1300 UT on 26 May 2006 is greater than that on 6 August 1999. It is noted that the different values of n , N , and ν_{in} between these two sampling days account for the difference of τ . Moreover, because the $2\pi\tau$ of 111 min is comparable to the observed period (20–40 min) of the nighttime MSTIDs on 6 August 1999, the MSTIDs could not propagate to the latitude of 25°N [Shiokawa et al., 2002]. In contrast, the $2\pi\tau$ of 416 min is not comparable to MSTIDs period in the night of 26 May 2006. This indicates that the ion-drag effect would not prevent the nighttime MSTIDs propagation in this day. It is noted that there would be possible uncertainties in the estimated values of τ , when the modeled data is adopted. However, some previous studies have used the modeled data of IRI-2001 and MSISE-90 to

compare the observed data, and have a good agreement [e.g., Chuo and Lee, 2008; Ding et al., 2003; Tsugawa et al., 2006]. Therefore, it would be acceptable to apply the data of these two models in this study.

[11] Figure 4 displays the time sequence of two-dimensional $|\Delta\text{TEC}/\text{min}|$ maps during 1440–1530 UT (2240–2330 LT) on 26 May 2006, with a 10-min interval. In Figure 4a, there are two band-like structures of the greater $|\Delta\text{TEC}/\text{min}|$ values (>0.2 TECU/min) which are located at about 121°E and 24°N , and at 119°E and 21.5°N . It is noted that the $|\Delta\text{TEC}/\text{min}|$ values greater than 0.2 TECU/min can signify that the irregularities of about 6 or longer kilometers scale present in the F region [Aarons et al., 1997; Mendillo et al., 2000]. For example, the relative vertical TEC (VTEC) and $\Delta\text{TEC}/\text{min}$ for the satellite PRN 19 pass observed by the CHYI (23.45°N , 120.14°E) GPS station during 1414–1708 UT are showed in Figure 5. In Figures 5b and 5c, it is found that the VTEC depletions and $|\Delta\text{TEC}/\text{min}| > 0.2$ TECU/min appear concurrently during about 1440–1600 UT. These results demonstrate that there are irregularities existing in the F region, and in turn causing the significant $|\Delta\text{TEC}/\text{min}|$ values during this period. Moreover, the 5×5 pixels smoothing method producing the two-dimensional map might reduce the value of $|\Delta\text{TEC}/\text{min}|$ enhancements, or cause uncertainty at one pixel. Therefore, we estimate the value of standard deviation for each pixel to examine the uncertainty. The values of standard deviation for all pixel in the two-dimensional $|\Delta\text{TEC}/\text{min}|$ maps are almost smaller than 0.08 TECU/min. Therefore, the uncertainty for each pixel would be acceptable.

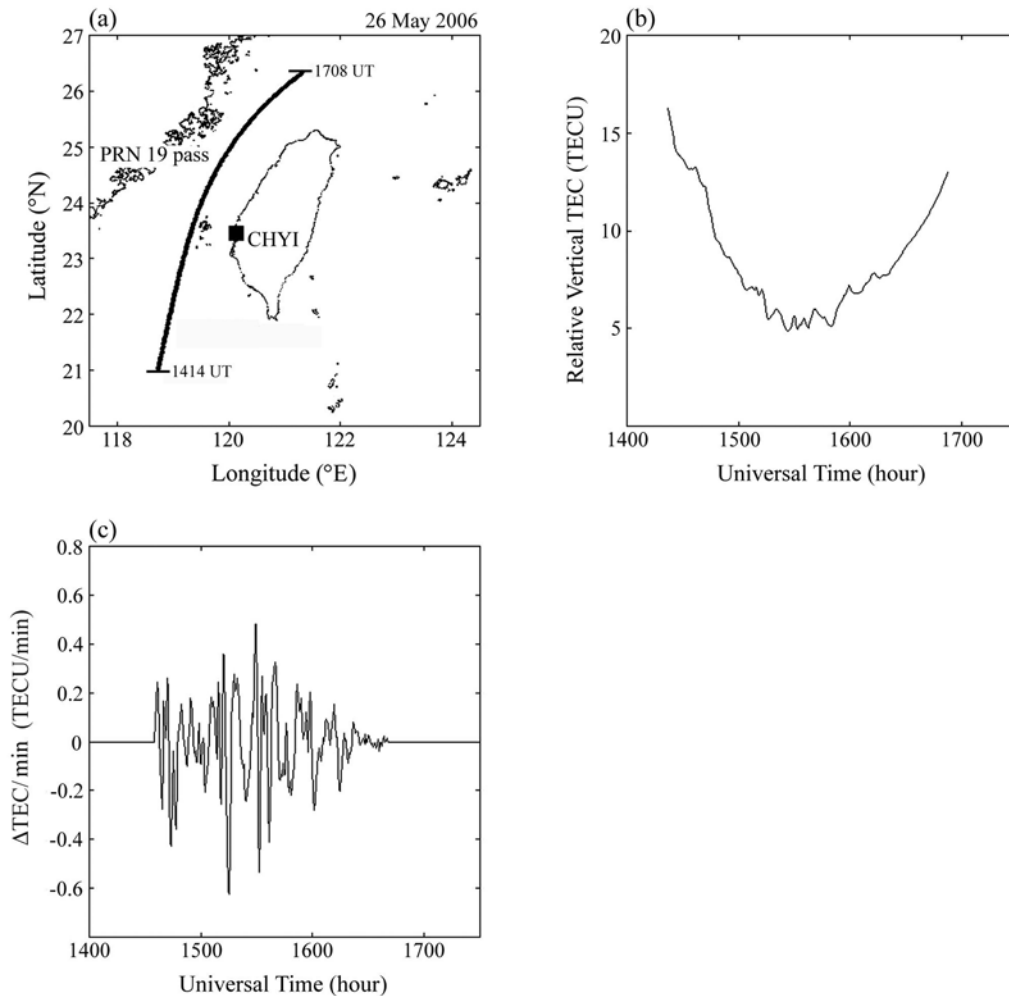


Figure 5. (a) The pass of GPS satellite PRN 19, as recorded by the CHYI station during 1414–1708 UT on 26 May 2006. The (b) relative vertical TEC and the (c) corresponding $\Delta\text{TEC}/\text{min}$ are plotted as a function of universal time.

[12] From 1440 to 1530 UT on 26 May 2006, these band-like greater $|\Delta\text{TEC}/\text{min}|$ structures move southwestward. Comparing with Figure 2, it is found that the band-like $|\Delta\text{TEC}/\text{min}|$ and wave-like TEC_p structures show a good agreement. Furthermore, that the F region irregularities of about 6 or longer kilometers scale are corresponding to the wave peak and trough of TEC_p . This result partially differs from that of *Saito et al.* [2002], in which the regions where the echoes from the 3-m scale F region irregularities were detected correspond to the peak and the northeastern slope of TEC_p . One possible explanation is that the scale size of F region irregularities observed by the GPS phase fluctuations ($|\Delta\text{TEC}/\text{min}|$) is different from that observed by the MU radar. The other might be the effect of the altitudinal distribution of F region irregularities. For GPS phase fluctuations, the magnitudes of $\Delta\text{TEC}/\text{min}$ are caused by all the F region irregularities along the GPS signal path. Accordingly, the altitudinal range of F region irregularities distribution is positively correlated with the magnitude of $|\Delta\text{TEC}/\text{min}|$ [*Chen et al.*, 2006]. Further, it is found that the coincidence between the TEC_p and $|\Delta\text{TEC}/\text{min}|$ structures indicates that both the MSTIDs and F region irregularities propagated southwestward at the same velocity, which is

similar to the results of *Saito et al.* [2002]. Furthermore, this coincidence demonstrates that the nighttime MSTIDs play an important role to generate F region irregularities in the low-latitude ionosphere on 26 May 2006.

4. Summary

[13] This study is the first attempt to study the nighttime MSTIDs occurring in the low-latitude ionosphere using the data of network GPS receivers in Taiwan, operated by NLSC. The two-dimensional mapping technique is applied on the TEC_p perturbations (TEC_p) to detect the MSTIDs features. Further, the same technique is applied on the GPS phase fluctuations ($|\Delta\text{TEC}/\text{min}|$) to examine the horizontal distribution of F region irregularities.

[14] On 26 May 2006, the nighttime MSTIDs moving southwestward with a horizontal velocity of 100–160 m/s and a wavelength of about 500 km are detected by the two-dimensional TEC_p maps. The wavefronts of MSTIDs structures are aligned along the northwest–southeast direction. Furthermore, the horizontal structures of MSTIDs observed by GPS network is similar to those observed by the Yonaguni airglows imager. These results demonstrate

that not only the nighttime MSTIDs can propagate to latitude of 20.5°N, but the two-dimensional TECp map is able to observe the MSTIDs in the low-latitude ionosphere.

[15] For the GPS phase fluctuations, the greater $|\Delta\text{TEC}/\text{min}|$ values in the two-dimensional $|\Delta\text{TEC}/\text{min}|$ map are corresponding to the wave peak and trough of TECp. Since the greater $|\Delta\text{TEC}/\text{min}|$ values represent that the plasma irregularities exist in the *F* region, this coincidence reveals that the MSTIDs play an important role for the generation of *F* region irregularities. This further indicates that the two-dimensional $|\Delta\text{TEC}/\text{min}|$ map can be utilized to monitor the horizontal distribution of *F* region irregularities.

[16] **Acknowledgments.** C.C.L. was supported by the grants of National Space Organization 97-NSPO(B)-SP-FA07-03(B), and National Science Council NSC 97-2119-M-231-001. Y.A.L. was supported by the grant of NSC 95-2111-M-008-011-MY3. The authors would like to thank the National Land Surveying and Mapping Center (NLSC), the Ministry of the Interior, Taiwan, for providing GPS data and the Center for Orbit Determination in Europe (CODE) for Global Ionosphere Maps (GIM).

[17] Zuyin Pu thanks the reviewers for their assistance in evaluating this paper.

References

- Aarons, J., M. Mendillo, and R. Yantosca (1997), GPS phase fluctuations in the equatorial region during sunspot minimum, *Radio Sci.*, *32*, 1535–1550, doi:10.1029/97RS00664.
- Bilitza, D. (2001), International Reference Ionosphere 2000, *Radio Sci.*, *36*, 261–275, doi:10.1029/2000RS002432.
- Chen, W. S., C. C. Lee, J. Y. Liu, F. D. Chu, and B. W. Reinisch (2006), Digisonde spread F and GPS phase fluctuations in the equatorial ionosphere during solar maximum, *J. Geophys. Res.*, *111*, A12305, doi:10.1029/2006JA011688.
- Chuo, Y. J., and C. C. Lee (2008), Ionospheric variability at Taiwan low latitude station: Comparison between observations and IRI-2001 model, *Adv. Space Res.*, *42*(4), 673–681, doi:10.1016/j.asr.2007.04.078.
- Ding, F., W. Wan, and H. Yuan (2003), The influence of background winds and attenuation on the propagation of atmospheric gravity waves, *J. Atmos. Sol. Terr. Phys.*, *65*, 857–869, doi:10.1016/S1364-6826(03)00090-7.
- Ding, F., W. Wan, B. Ning, and M. Wang (2007), Large-scale traveling ionospheric disturbances observed by GPS total electron content during the magnetic storm of 29–30 October 2003, *J. Geophys. Res.*, *112*, A06309, doi:10.1029/2006JA012013.
- Garcia, F. J., M. C. Kelley, J. J. Makela, and C.-S. Huang (2000), Airglow observations of mesoscale low-velocity traveling ionospheric disturbances at midlatitudes, *J. Geophys. Res.*, *105*, 18,407–18,415, doi:10.1029/1999JA000305.
- Hedin, A. E. (1991), Extension of the MSIS thermospheric model into the middle and lower atmosphere, *J. Geophys. Res.*, *96*, 1159–1172, doi:10.1029/90JA02125.
- Hernández-Pajares, M., J. M. Juan, and J. Sanz (2006), Medium-scale traveling ionospheric disturbances affecting GPS measurements: Spatial and temporal analysis, *J. Geophys. Res.*, *111*, A07S11, doi:10.1029/2005JA011474.
- Hines, C. O. (1972), *The Upper Atmosphere in Motion*, Heffernan, Worcester, Mass.
- Hunsucker, R. D. (1982), Atmospheric gravity waves generated in the high-latitude ionosphere: A review, *Rev. Geophys.*, *20*, 293–315, doi:10.1029/RG020i002p00293.
- Kotake, N., Y. Otsuka, T. Tsugawa, T. Ogawa, and A. Saito (2006), Climatological study of GPS total electron content variations caused by medium-scale traveling ionospheric disturbances, *J. Geophys. Res.*, *111*, A04306, doi:10.1029/2005JA011418.
- Kotake, N., Y. Otsuka, T. Ogawa, T. Tsugawa, and A. Saito (2007), Statistical study of medium-scale traveling ionospheric disturbances observed with the GPS networks in Southern California, *Earth Planets Space*, *59*, 95–102.
- Kubota, M., K. Shiokawa, M. K. Ejiri, Y. Otsuka, T. Ogawa, T. Sakanoi, H. Fukunishi, M. Yamamoto, S. Fukao, and A. Saito (2000), Traveling ionospheric disturbances observed in the OI 630-nm nightglow images over Japan by using a multipoint imager network during the FRONT campaign, *Geophys. Res. Lett.*, *27*(24), 4037–4040, doi:10.1029/2000GL011858.
- Liu, C. H., and K. C. Yeh (1969), Effect of ion drag on propagation of acoustic-gravity waves in the atmospheric F region, *J. Geophys. Res.*, *74*, 2248–2255, doi:10.1029/JA074i009p02248.
- Mannucci, A. J., B. A. Iijima, U. J. Lindqwister, X. Pi, L. Sparks, and B. D. Wilson (1999), GPS and ionosphere, in *Review of Radio Science 1996–1999*, edited by W. R. Stone, pp. 625–665, Int. Union for Radio Sci., Ghent, Belgium.
- Mendillo, M., B. Lin, and J. Aarons (2000), The application of GPS observations to equatorial aeronomy, *Radio Sci.*, *35*, 885–904, doi:10.1029/1999RS002208.
- Ogawa, T., N. Balan, Y. Otsuka, K. Shiokawa, C. Ihara, T. Shimomai, and A. Saito (2002), Observations and modeling of 630 nm airglow and total electron content associated with traveling ionospheric disturbances over Shigaraki, Japan, *Earth Planets Space*, *54*, 45–56.
- Ogawa, T., Y. Otsuka, K. Shiokawa, T. Tsugawa, A. Saito, K. Hoshino, K. Matunaga, M. Kubota, and M. Ishii (2008), Medium-scale traveling ionospheric disturbances and plasma bubbles observed by an all-sky airglow imager at Yonaguna, Japan, *Terr. Atmos. Oceanic Sci.*, in press.
- Otsuka, Y., K. Shiokawa, T. Ogawa, and P. Wilkinson (2004), Geomagnetic conjugate observations of medium-scale traveling ionospheric disturbances at midlatitude using all-sky airglow imagers, *Geophys. Res. Lett.*, *31*, L15803, doi:10.1029/2004GL020262.
- Otsuka, Y., F. Onoma, K. Shiokawa, T. Ogawa, M. Yamamoto, and S. Fukao (2007), Simultaneous observations of nighttime medium-scale traveling ionospheric disturbances and E region field-aligned irregularities at midlatitude, *J. Geophys. Res.*, *112*, A06317, doi:10.1029/2005JA011548.
- Perkins, F. (1973), Spread F and ionospheric currents, *J. Geophys. Res.*, *78*, 218–226, doi:10.1029/JA078i001p00218.
- Saito, A., S. Fukao, and S. Miyazaki (1998), High resolution mapping of TEC perturbations with the GSI GPS network over Japan, *Geophys. Res. Lett.*, *25*, 3079–3082, doi:10.1029/98GL52361.
- Saito, A., et al. (2001), Traveling ionospheric disturbances detected in the FRONT campaign, *Geophys. Res. Lett.*, *28*, 689–692, doi:10.1029/2000GL011884.
- Saito, A., N. Nishimura, M. Yamamoto, S. Fukao, T. Tsugawa, Y. Otsuka, S. Miyazaki, and M. C. Kelley (2002), Observations of traveling ionospheric disturbances and 3-m scale irregularities in the nighttime F region ionosphere with the MU radar and a GPS network, *Earth Planets Space*, *54*, 31–44.
- Shiokawa, K., Y. Otsuka, M. K. Ejiri, Y. Sahai, T. Kadota, C. Ihara, T. Ogawa, K. Igarashi, S. Miyazaki, and A. Saito (2002), Imaging observations of the equatorward limit of midlatitude traveling ionospheric disturbances, *Earth Planets Space*, *54*, 57–62.
- Shiokawa, K., C. Ihara, Y. Otsuka, and T. Ogawa (2003a), Statistical study of nighttime medium-scale traveling ionospheric disturbances using midlatitude airglow images, *J. Geophys. Res.*, *108*(A1), 1052, doi:10.1029/2002JA009491.
- Shiokawa, K., Y. Otsuka, C. Ihara, T. Ogawa, and F. J. Rich (2003b), Ground and satellite observations of nighttime medium-scale traveling ionospheric disturbance at midlatitude, *J. Geophys. Res.*, *108*(A4), 1145, doi:10.1029/2002JA009639.
- Shiokawa, K., et al. (2005), Geomagnetic conjugate observation of nighttime medium-scale and large-scale traveling ionospheric disturbances: FRONT3 campaign, *J. Geophys. Res.*, *110*, A05303, doi:10.1029/2004JA010845.
- Strobel, D. F., and M. B. McElroy (1970), The F2-layer at middle latitude, *Planet. Space Sci.*, *18*, 1181–1202, doi:10.1016/0032-0633(70)90211-4.
- Tsugawa, T., T. Sadakane, J. Sato, Y. Otsuka, T. Ogawa, K. Shiokawa, and A. Saito (2006), Summer-winter hemispheric asymmetry of sudden increase in ionospheric total electron content induced by solar flares: A role of O/N2 ratio, *J. Geophys. Res.*, *111*, A11316, doi:10.1029/2006JA011951.
- Tsugawa, T., Y. Otsuka, A. J. Coster, and A. Saito (2007), Medium-scale traveling ionospheric disturbances detected with dense and wide TEC maps over North America, *Geophys. Res. Lett.*, *34*, L22101, doi:10.1029/2007GL031663.
- Yokoyama, T., Y. Otsuka, T. Ogawa, M. Yamamoto, and D. L. Hysell (2008), First three-dimensional simulation of the Perkins instability in the nighttime midlatitude ionosphere, *Geophys. Res. Lett.*, *35*, L03101, doi:10.1029/2007GL032496.
- F. D. Chu, National Standard Time and Frequency Laboratory, Telecommunication Laboratories, Chunghwa Telecom Co., Ltd., Chung-Li, 320 Taiwan.
- K. Hoshino and K. Matunaga, Electronic Navigation Research Institute, Chofu, Tokyo 182-0012, Japan.
- C. C. Lee, General Education Center, Ching Yun University, Jongli, 320 Taiwan. (cclee@cyu.edu.tw)
- Y. A. Liou, Center for Space and Remote Sensing Research, National Central University, Chung-Li, 320 Taiwan.
- Y. Otsuka, Solar-Terrestrial Environment Laboratory, Nagoya University, Toyokawa, Aichi 442-8507, Japan.
- T. K. Yeh, Institute of Geoinformatics and Disaster Reduction Technology, Ching Yun University, Jongli, 320 Taiwan.